Alternating Copolymers Incorporating Cyclopenta[2,1-*b*:3,4-*b*′]dithiophene Unit and Organic Dyes for Photovoltaic Applications

YEN-JU CHENG, LUNG-CHANG HUNG, FONG-YI CAO, WEI-SHUN KAO, CHIH-YU CHANG, CHAIN-SHU HSU

Department of Applied Chemistry, National Chiao Tung University, 1001 Ta Hsueh Road, Hsin-Chu 30010, Taiwan

Received 4 January 2011; accepted 26 January 2011
DOI: 10.1002/pola.24604
Published online 4 March 2011 in Wiley Online Library (wileyonlinelibrary.com).

ABSTRACT: We have synthesized six p-type copolymers, **CPDT-*co*-TPADCN**, **CPDT-*co*-TPADTA**, **CPDT-*co*-TPATCN**, **CPDT-*co*-DFADCN**, **CPDT-*co*-DFADTA**, and **CPDT-*co*-DFATCN**, consisting of a cyclopenta[2,1-*b*:3,4-*b*′]dithiophene (CPDT) unit and an organic dye in an alternating arrangement. Triphenylamine (TPA) or difluorenylphenyl amine (DFA) units serve as the electron donors, whereas dicyanovinyl (DCN), 1,3-diethyl-2-thiobarbituric acid, or tricyanovinyl (TCN) units act as the electron acceptors in the dyes. The target polymers were prepared via Stille coupling, followed by postfunctionalization to introduce the electron acceptors to the side chains. Because of the strongest withdrawing ability of TCN acceptor to induce efficient intramolecular charge transfer, **CPDT-*co*-TPATCN** and **CPDT-*co*-DFATCN** exhibit the broader absorption spectra covering from 400 to 900 nm and the narrower optical band gaps of 1.34 eV. However, the **CPDT-*co*-TPATCN**:$PC_{71}BM$ and **CPDT-*co*-DFATCN**:$PC_{71}BM$ based solar cells showed the power conversion efficiencies (PCEs) of 0.22 and 0.31%, respectively, due to the inefficient exciton dissociation. The DFA-based polymers possess deeper-lying HOMO energy levels than the TPA-based polymer analogues, leading to the higher V_{oc} values and better efficiencies. The device based on **CPDT-*co*-DFADTA**:$PC_{71}BM$ blend achieved the best PCE of 1.38% with a V_{oc} of 0.7 V, a J_{sc} of 4.57 mA/cm^2, and a fill factor of 0.43. © 2011 Wiley Periodicals, Inc. J Polym Sci Part A: Polym Chem 49: 1791–1801, 2011

KEYWORDS: conjugated polymers; copolymerization; organic dyes; polycondensation; polymer solar cells

INTRODUCTION Polymer-based solar cells (PSCs) have attracted considerable interest in recent years because of their merits for lightweight and feasibility of coating on flexible surface by inexpensive solution processing. PSCs based on the concept of bulk heterojunction (BHJ) configuration where an active layer comprises a p-type (donor) and an n-type (acceptor) materials represent the most useful strategy to maximize the internal donor–acceptor interfacial area allowing for efficient charge separation.[1–5] Fullerene derivatives such as [6,6]-phenyl-C_{61}-butyric acid methyl ester (PCBM) is the most widely used n-type materials for BHJ solar cells because of their exceptional ability to induce ultrafast electron transfer and excellent electron transport properties.[6] To achieve high efficiency of PSCs, one of the most critical challenges in the molecular level is to develop ideal p-type conjugated polymers that possess (1) sufficient solubility to guarantee solution processability and miscibility with an n-type material, (2) low band-gap (LBG) for strong and broad absorption spectrum extending to near infrared to capture more solar photons, and (3) high hole mobility for efficient charge transport. Furthermore, positions of donor's highest occupied molecular orbital (HOMO) and lowest unoccupied molecular orbital (LUMO) levels are of critical importance; the HOMO energy level of the conjugated polymer must be low-lying for generating large open-circuit voltage (V_{oc}),[7–9] whereas the LUMO energy level must be at least 0.3 eV higher than the LUMO energy level of PCBM to afford efficient electron transfer.[10,11] The most powerful strategy to design a LBG conjugated polymer is to incorporate electron-rich donor and electron-deficient acceptor segments in the polymer backbone. On photo-excitation, efficient photoinduced intramolecular charge transfer (ICT) takes place from the donor to the acceptor, generating an absorption band at the lower energy. Based on this molecular strategy, a variety of important low-band-gap polymers with enhanced absorption abilities have appeared.[12–21]

Push/pull donor–π-bridge–acceptor (D–π–A) organic chromophores, comprising an electron-releasing donor unit, a π-conjugated bridge, and an electron-withdrawing acceptor unit, have been employed extensively and used as active materials in the field of nonlinear optics.[22,23] Because of the efficient photo-induced ICT taking place from the donor to acceptor, such chromophores are strong light-absorbing dyes possessing broad absorption window extending to near near-infrared region. Moreover, the optical properties of D–π–A chromophores can be easily fine-tuned by adjusting the donating strength of donor, withdrawing strength of acceptor or varying the effective conjugated length of the bridge in the dye.[24,25] Based on these intrinsic advantages, D–π–A chromophores have also been used as effective light-

Additional Supporting Information may be found in the online version of this article. Correspondence to: Y.-J. Cheng (E-mail: yjcheng@mail.nctu.edu.tw) or C.-S. Hsu (E-mail: cshsu@mail.nctu.edu.tw)

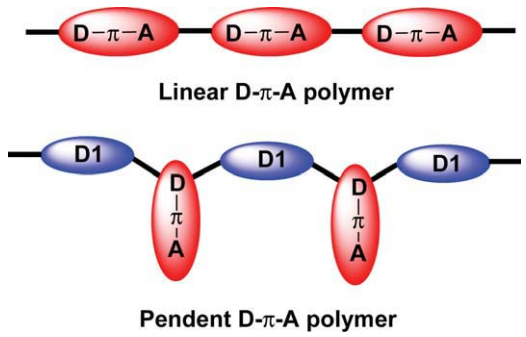

SCHEME 1 The structures of linear D–π–A polymer and pendent D–π–A polymer. [Color figure can be viewed in the online issue, which is available at wileyonlinelibrary.com.]

harvesting dyes in dye-sensitized solar cells.[26–31] It is envisaged that incorporation of D–π–A organic dyes into p-type conjugated polymers might be a useful strategy to improve the light-harvesting and charge transporting properties. As shown in Scheme 1, there are generally two design strategies to prepare D–π–A type polymer. One is one-dimensional linear D–π–A polymer and the other is two-dimensional pendent D–π–A polymer. However, it is synthetically challenging to form a linear D–π–A polymer in a head-to-tail manner without seriously disrupting main chain conjugation (Scheme 1). A more practical way is to construct the main chain by copolymerizing the donor unit of the dye with an electron-rich conjugated moiety (D1; Scheme 1). In this manner, the donor unit of the dye is embedded into the polymer backbone, whereas the π-bridge and acceptor of the dye become the pendent group that is perpendicular to the main chain. Recently, several new conjugated polymers with pendent D–π–A side chains have been reported for the use in PSCs.[32–36] Triphenylamino (TPA) and vinylene thiophene groups serve as the donor and π-conjugated bridge, respectively, whereas dicyanovinyl and 1,3-diethyl-2-thiobarbituric acid (DTA) groups have been used as the acceptors in the dye. On the other hand, 2,7-fluorene,[32] silafluorene,[33] and carbazole[34–36] units have been used as the electron-rich groups (D1) to connect with dyes in the polymer main chain.

To further modulate the intrinsic properties of the pendent D–π–A polymers to optimal level for the applications of PSCs, exploration of new D1 group in the main chain as well as D and A groups in the dye is necessary. 4*H*-cyclopenta[2,1-*b*:3,4-*b*′]dithiophene (CPDT),[37] where a 2,2′ bithiophene is covalently bridged and rigidified at the 3,3′ position by a carbon and a silicon atom, respectively, has attracted considerable research interest owing to their potential to serve as donor building blocks for LBG polymers. Because of the fully coplanar structure, the intrinsic properties based on bithiophene can be altered, leading to more extended conjugation, lower HOMO–LUMO energy band-gap, and stronger intermolecular interaction. Furthermore, the ability of functionalization at bridging carbon and silicon allows for introducing two highly solubilizing aliphatic side chains without affecting its coplanarity. Poly[2,6-(4,4-bis(2-ethylhexyl)-4*H*-cyclopenta[2,1-*b*;3,4-*b*′]dithiophene)-*alt*-4,7-(2,1,3-benzothiadiazole)] using CPDT as the donor and benzothiadiazole as the acceptor represents one of the most promising LBG polymers for the use in PSCs.[38] In this article, we have successfully synthesized a series of newly designed alternating D–π–A pendent copolymers. CPDT is chosen to serve as the D1 group for all the polymers. Two different donor moieties, TPA and difluorenylphenyl amino (DFA) groups, are connected with three different acceptor units, dicyanovinyl (DCN), DTA, and tricyanovinyl (TCN) through the vinylene thiophene bridge, yielding six D–π–A pendant copolymers, denoted as **CPDT-*co*-TPADCN**, **CPDT-*co*-TPADTA**, **CPDT-*co*-TPATCN**, **CPDT-*co*-DFADCN**, **CPDT-*co*-DFADTA**, and **CPDT-*co*-DFATCN** (Scheme 2). The characterization and photovoltaic applications of these polymers will be discussed.

EXPERIMENTAL

Measurement and Characterization

All chemicals are purchased from Aldrich or Acros and used as received unless otherwise specified. ^{1}H NMR and ^{13}C NMR spectra were measured using Varian 300 MHz instrument spectrometer. The differential scanning calorimetry (DSC) measurement performed on TA Q200 Instrument and thermogravimetric analysis (TGA) was recorded on Perkin-Elmer Pyris under a nitrogen atmosphere at a heating rate of 10 °C/min. Absorption spectra were taken on a HP8453 UV–vis spectrophotometer. The molecular weight of polymers was measured by gel permeation chromatography (GPC) (Viscotek VE2001GPC) using a Waters Styragel column (concentration: 2 mg/1mL in tetrahydrofuran (THF); flow rate: 1 mL/1 min), and polystyrene was used as the standard (THF as the eluent). The cyclic voltammograms (CV) was conducted on a Bioanalytical System analyzer. A carbon glass coated with a thin polymer film was used as the working electrode and an Ag/AgCl as the reference electrode, whereas 0.1 M tetrabutylammonium hexafluorophosphate in acetonitrile was the electrolyte. The curves of CV were calibrated using ferrocene as the standard, whose oxidation potential is set at −4.8 eV with respect to zero vacuum level.

Fabrication of Photovoltaic Devices

ITO (indium tin oxide)/glass substrates were cleaned sequentially in the ultrasonic bath of detergent, deionized water, acetone, and isopropyl alcohol for 15 min. Then, the substrates were covered by a 30-nm thick layer of poly(3,4-ethylenedioxythiophene):poly(styrenesulfonate)(PEDOT:PSS, Al 4083 provided by H. C. Stark) by spin-coating. After annealing in air at 150 °C for 30 min, the samples were cooled down to room temperature.

All the polymers were dissolved in *ortho*-dichlorobenzene (0.5 wt %), and [6,6]-phenyl-C_{71}-butyric acid methyl ester ($PC_{71}BM$, purchased from Nano-C) was added to reach the desired ratio. The solution was then heated at 70 °C for 1 h and stirred overnight at room temperature. Before deposition, the solution was filtrated through a 0.45-μm filter, and the substrate was transferred in a glovebox. The active layer was then spin-coated at different spin rate to tune the thickness. After drying, the sample (**CPDT-*co*-TPATCN**/$PC_{71}BM$) was annealed at 150 °C for 10 min and other devices were not annealed. The spin rate for the sample (**CPDT-*co*-TPADTA**/$PC_{71}BM$) is 1500 rpm and for other

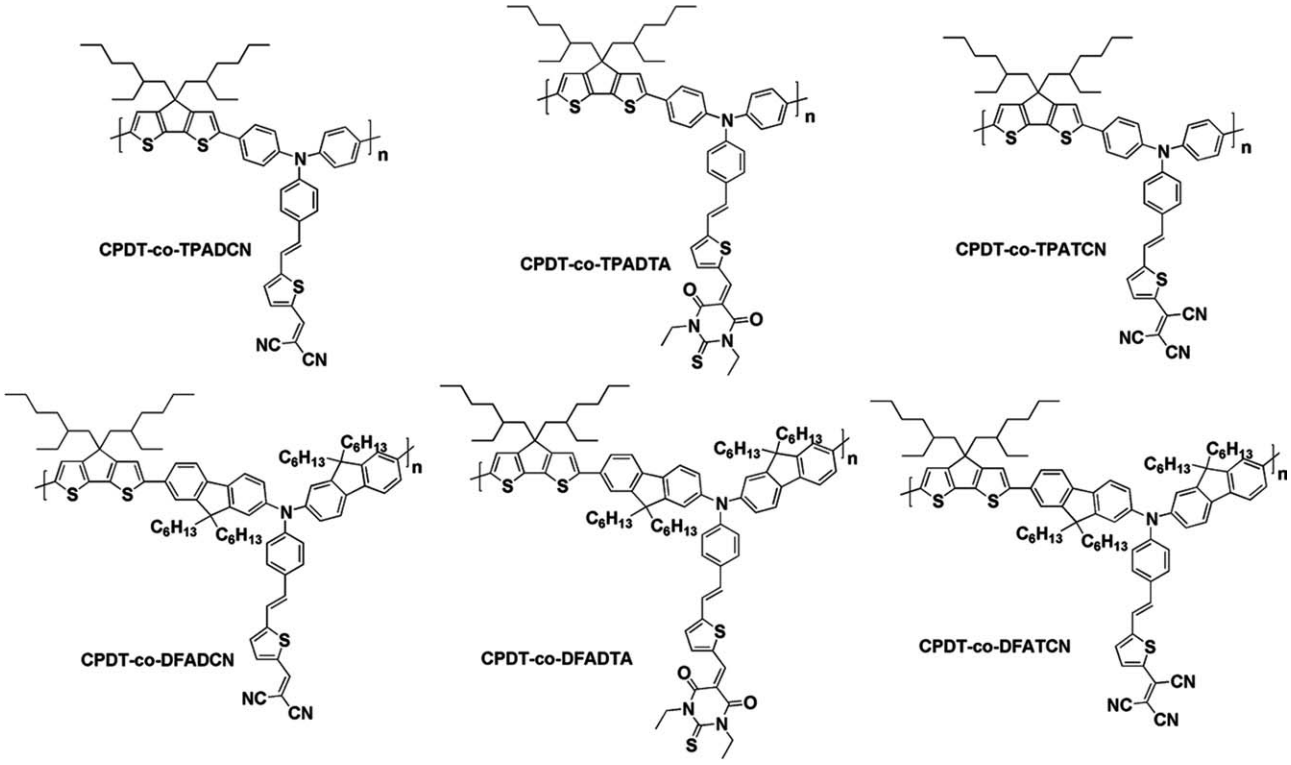

SCHEME 2 Chemical structures of the six polymers in this research.

samples is 1000 rpm (thickness = ~75–80 nm). The cathode made of calcium (35 nm) and aluminum (100 nm) was evaporated through a shadow mask under vacuum ($<10^{-6}$ Torr). Finally, the devices were encapsulated, and *J–V* curves were measured in air. Each device is constituted of 4 pixels defined by an active area of 0.04 cm^2.

Characterization of Photovoltaic Devices

The devices were characterized under the irradiation of AM 1.5 simulated light with intensity 100 mW/cm^2. Solar illumination conforming the JIS Class AAA was provided by a SAN-EI Electric 300 W solar simulator equipped with an AM 1.5G filter. The light intensity was calibrated with a Hamamatsu S1336-5BK silicon photodiode. Current-voltage (*J–V*) characteristics of PSC devices were obtained by a Keithley 2400 sourcemeter. The performances presented here are the average of the 4 pixels of each device.

Hole-Only Devices

To investigate the respective hole mobility of the different copolymer films, unipolar devices have been prepared following the same procedure, except that the active layer is made of pure polymer and the Ca/Al cathode is replaced by evaporated gold (10 nm) and silver (150 nm).

Synthesis of Monomers and Polymers

9,9-Dihexyl-2-bromofluorene (2)

A mixture of **1** (10 g, 40.8 mmol), *n*-hexyl bromide (15.5 g, 93.8 mmol), and 50% $NaOH_{(aq)}$ (60 mL) in THF (120 mL) was stirred at 80 °C for 12 h under nitrogen atmosphere. After cooling to room temperature, the resulting mixture was extracted with ether (50 mL × 3) and water. The combined organic layers were washed with water, dried over anhydrous $MgSO_4$, filtered, and the solvent was removed by evaporation. The crude product was then purified by column chromatography on silica gel using hexane as eluent to afford the desired product **2** as a colorless liquid (16.6 g, 89%).

^{1}H NMR (300 MHz, $CDCl_3$): δ7.67–7.64 (m, 1H), 7.56–7.53 (m, 1H), 7.45–7.42 (m, 2H), 7.32–7.30 (m, 3H), 1.93 (m, 4H), 1.12–1.04 (m, 12H), 0.79–0.74 (m, 6H), 0.59 (t, J = 6.6 Hz, 4H).

9,9-Dihexyl-2-bromo-7-iodofluorene (3)

A mixture of **2** (3 g, 7.26 mmol), iodine (1.11 g, 4.35 mmol), concentrated sulfuric acid (1 mL), periodic acid (0.99 g, 4.35 mmol), and water (5 mL) in glacial acetic acid (110 mL) was stirred at 80 °C for 12 h. After cooling to room temperature, the solution was poured into ice-cooled water containing sodium sulfite, and the resulting mixture was extracted with ethyl acetate (50 mL × 3). The combined organic phases were washed twice with water, dried over anhydrous $MgSO_4$, and the solvent was removed by evaporation. The crude product was then purified by column chromatography on silica gel using hexane as eluent to afford the desired product **3** as a light-yellow liquid (3.16 g, 81%).

^{1}H NMR (300 MHz, $CDCl_3$): δ 7.65–7.63 (m, 2H), 7.52–7.50 (m, 1H), 7.45–7.38 (m, 3H), 1.93–1.87 (m, 4H), 1.15–1.03 (m, 12H), 0.80–0.75 (m, 6H), 0.60–0.53 (m, 4H).

N,N-*Di(7-bromo-9,9-dihexyl-2-fluorenyl)*-N-*phenylamine (4)*

A mixture of **7** (8.4 g, 15.6 mmol), aniline (0.66 g, 7.08 mmol), copper(I) chloride (0.18 g, 1.77 mmol), potassium

hydroxide (3.18 g, 56.6 mmol), and 1,10-phenanthroline (0.32 g, 1.77 mmol) in toluene (120 mL) was stirred at 125 °C for 12 h under nitrogen atmosphere. After cooling to room temperature, the mixture was extracted with ethyl acetate (50 mL × 3) and brine water, and then the combined organic layers dried over anhydrous $MgSO_4$ and filtered, and the solvent was removed by evaporation. The crude product was purified by column chromotography on silica gel using hexane as eluent to afford the desired product **4** as a light-yellow solid (3.1 g, 48%).

^{1}H NMR (300 MHz, $CDCl_3$): δ 7.44–7.32 (m, 8H), 7.20–7.15 (m, 2H), 7.06–7.04 (m, 4H), 6.97–6.92 (m, 3H), 1.76 (t, J = 5.9 Hz, 8H), 1.09–1.04 (m, 24H), 0.78–0.70 (m, 12H), 0.56 (m, 8H).

4-[Bis(2-bromo-9,9-dihexyl-7-fluorenyl) amino]benzaldehyde (5)

To a solution of **4** (0.95 g, 1.04 mmol) and *N,N*-dimethylformamide (DMF) (0.76 g, 10.4 mmol) in 1,2-dichloroethane was added $POCl_3$ (1.59 g, 10.4 mmol) by syringe at 0 °C. The mixture was stirred at 90 °C for 12 h. After being cooled to room temperature, the solution was poured into $NaHCO_3$ solution slowly and stirred for 30 min. The mixture was extracted with CH_2Cl_2 and water; the combined organic layers were dried over $MgSO_4$, evaporated, and purified with column chromatography [silica gel, hexane/ethyl acetate (20/1) as eluent] to yield **5** as yellow liquid (0.77 g, 79%).

MS (FAB) m/z: 944. ^{1}H NMR (300 MHz, $CDCl_3$): δ 9.84 (s, 1H), 7.70 (d, J = 8.7 Hz, 2H), 7.60 (d, J = 8.1 Hz, 2H), 7.52–7.43 (m, 6H), 7.20 (m, 2H), 7.12–7.08 (m, 4H), 1.90–1.85 (m, 8H), 1.81–1.06 (m, 24H), 0.84–0.76 (m, 12H), 0.66 (m, 8H); ^{13}C NMR (75 MHz, $CDCl_3$): δ 190.3, 153.3, 153.0, 152.1, 145.6, 139.4, 137.2, 131.3, 130.1, 129.2, 126.1, 125.1, 120.9, 120.8, 120.7, 119.4.

7-Bromo-N-(2-bromo-9,9-dihexyl-7-fluorenyl)-9,9-dihexyl-N-[4-[2-(thio-phen-2-yl)vinyl]phenyl]fluoren-2-amine (M3)

To a solution of **5** (0.3 g, 0.32 mmol) and diethyl (2-methylthiophene)-phosphonate **6** (0.09 g, 0.39 mmol) in dry THF (50 mL) was added potassium *tert*-butoxide methanol solution (1 M, 0.4 mL). The reaction mixture was stirred for 12 h at room temperature and then was neutralized with 5% hydrochloric acid solution. The two phases were separated, and the water phase was extracted twice with dichloromethane. The combined organic extracts were washed three times with water, dried over $MgSO_4$, evaporated, and purified with column chromatography on silica gel using hexane/ethyl acetate (20/1) as eluent to yield **M3** as a yellow solid (0.26 g, 80%).

MS (FAB) m/z: 1024. ^{1}H NMR (300 MHz, $CDCl_3$): δ 7.54–7.51 (m, 2H), 7.48 (s, 1H), 7.45–7.41 (m, 5H), 7.36–7.33 (m, 2H), 7.17–7.15 (m, 3H), 7.11–6.97 (m, 7H), 6.92–6.87 (m, 1H), 1.85 (t, J = 6.6 Hz, 8H), 1.18–1.07 (m, 25H), 0.84–0.78 (m, 11H), 0.66 (m, 8H); ^{13}C NMR (75 MHz, $CDCl_3$): δ 152.8, 151.8, 147.3, 147.0, 143.2, 139.8, 135.4, 131.1, 129.9, 127.7, 127.6, 127.1, 126.0, 125.6, 123.9, 123.5, 123.2, 120.5, 120.4, 120.3, 119.0. Anal. Calcd. for $C_{62}H_{73}Br_2NS$: C, 72.71; H, 7.18; N, 1.37. Found: C, 72.87; H, 7.32; N, 1.31.

5-[4-[Bis(2-bromo-9,9-dihexyl-7-fluorenyl)amino] styryl]thiophene-2-carbaldehyde (M4)

To a solution of **M3** (1.67 g, 1.63 mmol) and DMF (0.3 g, 4.08 mmol) in 1,2-dichloroethane was added $POCl_3$ (0.63 g, 4.08 mmol) by syringe at 0 °C. The mixture was stirred at 90 °C for 12 h. After being cooled to room temperature, the solution was poured into $NaHCO_3$ solution slowly and stirred for 30 min. The mixture was extracted with CH_2Cl_2 and water; the combined organic layers were dried over $MgSO_4$, evaporated, and purified with column chromatography [silica gel, hexane/ethyl acetate (20/1) as eluent] to yield **M4** as orange solid (2.73 g, 89%).

MS (FAB) m/z: 1052. ^{1}H NMR (300 MHz, $CDCl_3$): δ 9.85 (s, 1H), 7.66 (d, J = 3.6 Hz, 1H), 7.56–7.53 (m, 2H), 7.50–7.42 (m, 6H), 7.38–7.35 (m, 2H), 7.15–7.03 (m, 9H), 1.87–1.83 (m, 8H), 1.17–1.07 (m, 24H), 0.86–0.79 (m, 11H), 0.66 (m, 9H): ^{13}C NMR (75 MHz, $CDCl_3$): δ 182.2, 152.9, 152.7, 151.8, 148.4, 146.5, 140.9, 139.6, 137.3, 135.7, 132.3, 129.9, 129.4, 127.8, 125.9, 123.8, 122.4, 120.5, 120.4, 119.3, 118.7, 55.2, 40.0, 31.4, 29.5, 23.7, 22.5, 14.0. Anal. Calcd. for $C_{63}H_{73}Br_2NOS$: C, 71.92; H, 6.99; N, 1.33. Found: C, 71.86; H, 7.27; N, 1.36.

General Procedure for the Synthesis of Conjugated Precursor Polymers via Stille Coupling Reaction

Into a 25-mL of two-neck flask, 1 equiv of dibromo monomers (**M1**–**M4**) and 1 equiv of **M5**, $Pd_2(dba)_3$ (4 mol %) and tri(*o*-tolyl)phosphine (32 mol %) were added in anhydrous toluene and deoxygenated with nitrogen for 30 min. The reaction mixture was stirred at 120 °C for 3 days. After cooling to room temperature, the solution was added into methanol dropwise. The precipitate was collected by filtration and washed by Soxhlet extraction with methanol, acetone, and THF sequentially for 3 days. The Pd-thiol gel (Silicycle) was added to above THF solution to remove the residual Pd catalyst. After filtration and removal of the solvent, the polymer was redissolved in THF again and added into methanol to reprecipitate out. The purified polymer was collected by filtration and dried under vacuum for 1 day.

CPDT-co-*TPA*

Following the general polymerization procedure, **M5** (659 mg, 0.905 mmol), **M1** (463 mg, 0.905 mmol), $Pd_2(dba)_3$ (33.2 mg, 0.036 mmol), P(*o*-tolyl)$_3$ (88.2 mg, 0.29 mmol), and toluene (30 mL) were used in the polymerization, and the polymer was obtained as a orange powder (0.34 g, 50%).

^{1}H NMR (300 MHz, $CDCl_3$): δ 7.51–7.49 (m, 4H), 7.40–7.36 (m, 2H), 7.20–7.13 (m, 9H), 7.06–7.05 (m, 2H), 7.02–7.00 (m, 1H), 6.93–6.87 (m, 1H), 1.91 (m, 4H), 1.00–0.98 (m, 16H), 0.74 (m, 8H), 0.65 (t, J = 7.2 Hz, 6H).

CPDT-co-*TPACHO*

Following the general polymerization procedure, **M5** (333.5 mg, 0.458 mmol), **M2** (246.9 mg, 0.458 mmol), $Pd_2(dba)_3$ (16.8 mg, 0.018 mmol), P(*o*-tolyl)$_3$ (44.6 mg, 0.147 mmol), and toluene (15 mL) were used in this polymerization, and

the polymer was obtained as a orange powder (0.31 g, 86%).

^{1}H NMR (300 MHz, $CDCl_3$): δ 9.85 (s, 1H), 7.67–7.66 (m, 1H), 7.53–7.50 (m, 4H), 7.43–7.40 (m, 2H), 7.14–7.12 (m, 11H), 1.91 (m, 4H), 1.01–0.99 (m, 16H), 0.74 (m, 7H), 0.68–0.63 (m, 7H).

CPDT*-co-*DFA

Following the general polymerization procedure, **M5** (287 mg, 0.394 mmol), **M3** (404 mg, 0.394 mmol), $Pd_2(dba)_3$ (14.4 mg, 0.016 mmol), P(*o*-tolyl)$_3$ (38.4 mg, 0.126 mmol), and toluene (13 mL) were used in this polymerization, and the polymer was obtained as an orange powder (0.261 g, 52%).

^{1}H NMR (300 MHz, $CDCl_3$): δ 7.61–7.59 (m, 4H), 7.51 (m, 2H), 7.33 (m, 3H), 7.20 (m, 4H), 7.12–6.88 (m, 10H), 1.95 (m, 12H), 1.11 (m, 40H), 0.82–0.80 (m, 14H), 0.71–0.69 (m, 20H).

CPDT*-co-*DFACHO

Following the general polymerization procedure, **M5** (240 mg, 0.33 mmol), **M4** (347 mg, 0.33 mmol), $Pd_2(dba)_3$ (12.1 mg, 0.013 mmol), P(*o*-tolyl)$_3$ (32.1 mg, 0.106 mmol), and toluene (11 mL) were used in this polymerization, and the polymer was obtained as a orange-red powder (0.282 g, 66%).

^{1}H NMR (300 MHz, $CDCl_3$): δ 9.85 (s, 1H), 7.67–7.66 (m, 1H), 7.61–7.58 (m, 6H), 7.51 (m, 2H), 7.40–7.37 (m, 2H), 7.21 (m, 2H), 7.07 (m, 9H), 1.97 (m, 12H), 1.22–1.05 (m, 44H), 0.85–0.80 (m, 17H), 0.71–0.67 (m, 13H).

Post Functionalization of the Polymer Precursors

CPDT*-co-*TPADCN

To a solution of **CPDT-*co*-TPACHO** (89.7 mg, 0.115 mmol) and malononitrile (0.27 g, 4.01 mmol) in chloroform (10 mL) was added pyridine (0.5 mL). The mixture solution was stirred for 16 h at room temperature. The resulting mixture was poured into methanol and the precipitate was filtered off and washed with water. The resulting polymer was dissolved in THF and precipitated again in methanol to afford black solid (74.6 mg, 78%).

^{1}H NMR (300 MHz, $CDCl_3$): δ 7.74 (s, 1H), 7.61–7.60 (m, 1H), 7.54–7.52 (m, 4H), 7.44–7.41 (m, 2H), 7.20–7.15 (m, 10H), 1.93 (m, 4H), 1.01–0.99 (m, 16H), 0.75 (m, 8H), 0.65 (t, J = 7.2 Hz, 6H). GPC (THF, polystyrene standard) M_n = 9.4 × 10^3 g/mol, M_w = 2.3 × 10^4 g/mol, PDI (polydispersity index) = 2.44.

CPDT*-co-*TPADTA

To a solution of **CPDT-*co*-TPACHO** (170 mg, 0.217 mmol) and DTA (1.52 g, 7.61 mmol) in 10 mL, chloroform was added to pyridine (0.5 mL). The mixture solution was stirred for 16 h at room temperature. The resulting mixture was poured into methanol, and the precipitate was filtered off and washed with water. The resulting polymer was dissolved in THF and precipitated again in methanol to afford black green solid (198 mg, 94%).

^{1}H NMR (300 MHz, $CDCl_3$): δ 8.63 (s, 1H), 7.80 (m, 1H), 7.61–7.37 (m, 7H), 7.20–7.16 (m, 10H), 4.60 (m, 4H), 1.92 (m, 4H), 1.36–1.20 (m, 6H), 1.01 (m, 16H), 0.75 (m, 8H), 0.66 (m, 6H). GPC (THF, polystyrene standard) M_n = 5.5 × 10^3 g/mol, M_w = 9.8 × 10^3 g/mol, PDI = 1.79.

CPDT*-co-*TPATCN

To a 25-mL two-necked flask containing the polymer **CPDT-*co*-TPA** (0.15 g, 0.199 mmol) and anhydrous DMF (10 mL) was added tetracyanoethylene (TCNE; 0.13 g, 0.994 mmol). The color of the solution rapidly changed to dark-green. The reaction mixture was heated at 85 °C for 24 h and then cooled to room temperature. The resulting solution was added into methanol dropwise to give a dark-green solid. The resulting polymer was dissolved in THF and precipitated again in methanol to afford dark-green solid (58.5 mg, 34%).

^{1}H NMR (300 MHz, $CDCl_3$): δ 7.97 (m, 1H), 7.55 (m, 3H), 7.46–7.43 (m, 3H), 7.24–7.23 (m, 2H), 7.16 (m, 7H), 1.93 (m, 4H), 1.01 (m, 15H), 0.74 (m, 7H), 0.68–0.66 (m, 8H). GPC (THF, polystyrene standard) M_n = 6.95× 10^3 g/mol, M_w = 1.15 × 10^4 g/mol, PDI = 1.66.

CPDT*-co-*DFADCN

To a solution of **CPDT-*co*-DFACHO** (156 mg, 0.12 mmol) and malononitrile (0.28 g, 4.21 mmol) in chloroform (10 mL) was added pyridine (0.5 mL). The mixture solution was stirred for 16 h at room temperature. The resulting mixture was poured into methanol, and the precipitate was filtered off and washed with water. The resulting polymer was dissolved in THF and precipitated again in methanol to afford black green solid (141 mg, 87%).

^{1}H NMR (300 MHz, $CDCl_3$): δ 7.74 (s, 1H), 7.61–60 (m, 8H), 7.52 (m, 3H), 7.41–7.39 (m, 3H), 7.21–7.19 (m, 3H), 7.13–7.08 (m, 5H), 1.97 (s, 12H), 1.11–1.05 (m, 42H), 0.84–0.80 (m, 17H), 0.71–0.67 (m, 15H). GPC (THF, polystyrene standard) M_n = 1.13× 10^4 g/mol, M_w = 3.29 × 10^4 g/mol, PDI = 2.92.

CPDT*-co-*DFADTA

To a solution of **CPDT-*co*-DFACHO** (177 mg, 0.137 mmol) and DTA (0.96 g, 4.79 mmol) in chloroform (10 mL) was added pyridine (0.5 mL). The mixture solution was stirred for 16 h at room temperature. The resulting mixture was poured into methanol and the precipitate was filtered off and washed with water. The resulting polymer was dissolved in THF and precipitated again in methanol to afford black green solid (180 mg, 89%).

^{1}H NMR (300 MHz, $CDCl_3$): δ 8.63 (s, 1H), 7.80 (m, 1H), 7.61–7.59 (m, 7H), 7.51 (m, 3H), 7.44–7.41 (m, 3H), 7.22–7.08 (m, 8H), 4.61 (m, 4H), 1.96 (m, 12H), 1.36–1.22 (m, 12H), 1.11 (m, 40H), 0.82–0.80 (m, 16H), 0.71–0.69 (m, 12H). GPC (THF, polystyrene standard) M_n = 4.41× 10^3 g/mol, M_w = 9.97 × 10^3 g/mol, PDI = 2.26.

CPDT*-co-*DFATCN

To a 25-mL two-necked flask containing the polymer **CPDT-*co*-DFA** (0.247 g, 0.195 mmol) and anhydrous DMF (10 mL) was added TCNE (0.1 g, 0.78 mmol). The color of the solution rapidly changed to dark-green. The reaction mixture was heated at 85 °C for 24 h and then cooled to room

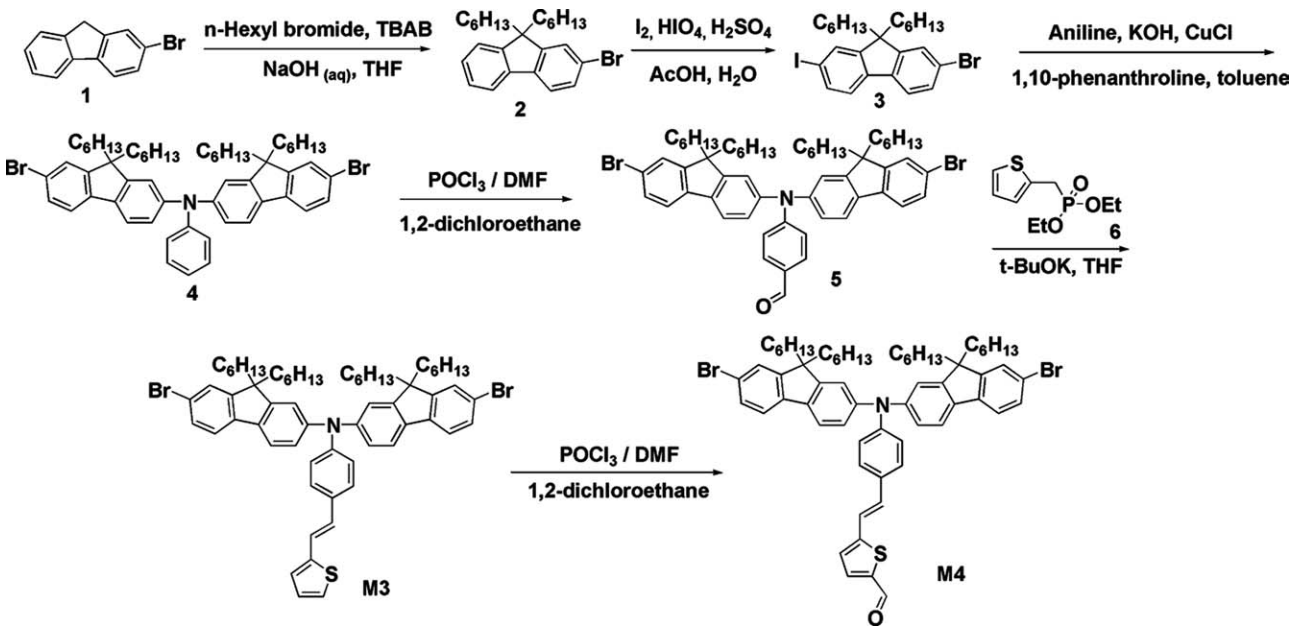

SCHEME 3 Synthesis of monomers **M3** and **M4**.

temperature. The resulting solution was added into methanol dropwise to give a dark-green solid. The resulting polymer was dissolved in THF and precipitated again in methanol to afford black green solid (115 mg, 43%).

^{1}H NMR (300 MHz, $CDCl_3$): δ 7.97 (d, J = 4.5 Hz, 1H), 7.63–7.61 (m, 6H), 7.52 (m, 2H), 7.44–7.41 (m, 3H), 7.33 (m, 1H), 7.21–7.20 (m, 3H), 7.15–7.10 (m, 6H), 1.97 (m, 12H), 1.11 (m, 41H), 0.84–0.79 (m, 17H), 0.71–0.69 (m, 16H). GPC (THF, polystyrene standard) M_n = 6.81× 10^3 g/mol, M_w = 1.56 × 10^4 g/mol, PDI = 2.30.

RESULTS AND DISCUSSION

Synthesis

The synthesis of monomers **M1** and **M2** were synthesized according to the literature,[32] and the synthetic route for **M3** and **M4** is shown in Scheme 3. Double alkylation of the 2-bromofluorene **1** in the presence of sodium hydroxide, tetrabutylammonium bromide (TBAB), and *n*-hexylbromide afforded compound **2**. Iodination of **2** with periodic acid/I_2 yielded compound **3**, which was then coupled with aniline via Ullmann coupling to afford DFA **4**. Formylation of

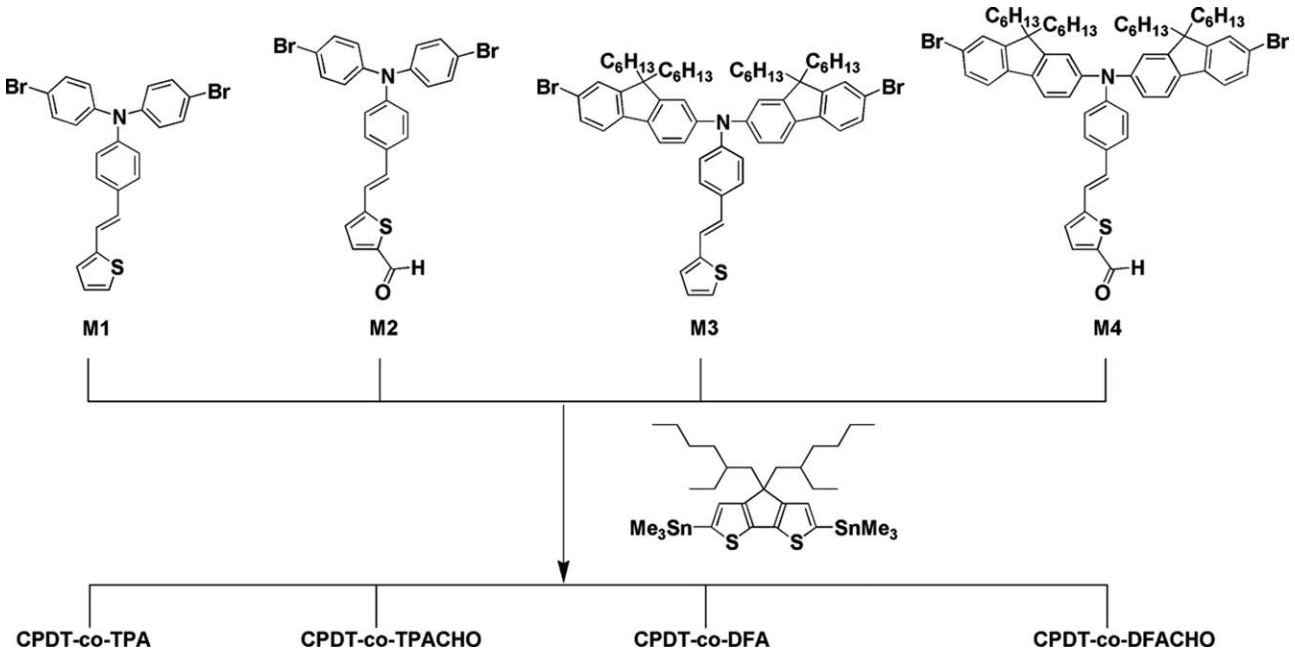

SCHEME 4 Synthesis of the precursor polymers by Stille coupling.

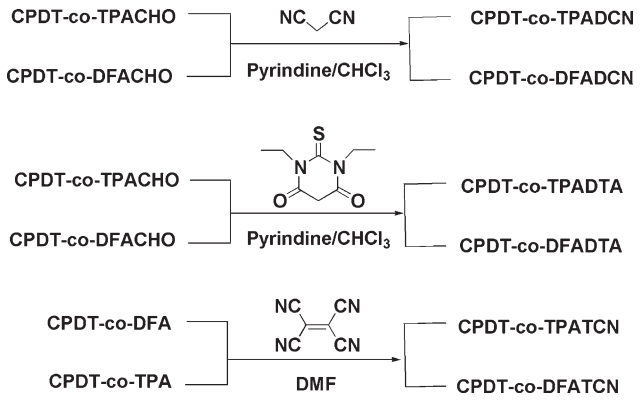

SCHEME 5 Synthesis of the target polymers by postfunctionalization.

compound **4** with phosphorus oxychloride and DMF under Vilsmeier reaction condition, followed by hydrolyzing the intermediates afforded compound **5**. Horner-Emmons reaction of **5** with diethyl (2-thienyl)methanephosphonate **6**[7] using potassium *tert*-butoxide as the base gave **M3**, which was then formylated via Vilsmeier reaction at 5-position to afford monomer **M4**.

As shown in Scheme 4, the precursor polymers, **CPDT-*co*-TPA**, **CPDT-*co*-TPACHO**, **CPDT-*co*-DFA**, and **CPDT-*co*-DFACHO**, were first synthesized by Stille polymerization of the distannyl-CPDT with **M1**, **M2**, **M3**, and **M4**, respectively, in presence of Pd_2dba_3/P(*o*-tolyl)$_3$ as the catalyst. Finally, the D–π–A chromophores in the target polymers were completed by the postfunctionalization to attach the acceptor, as shown in Scheme 4. The aldehyde groups in **CPDT-*co*-TPACHO** and **CPDT-*co*-DFACHO** polymers were condensed with malononitrile or DTA via Knoevenagel reaction to yield the target polymers, **CPDT-*co*-TPADCN**, **CPDT-*co*-TPADTA**, **CPDT-*co*-DFADCN**, and **CPDT-*co*-DFADTA**, respectively, whereas **CPDT-*co*-TPA** and **CPDT-*co*-DFA** polymers were reacted with TCNE to afford the corresponding polymers, **CPDT-*co*-TPATCN** and **CPDT-*co*-DFATCN** (Scheme 5).[39] The ^{1}H NMR and ^{13}C NMR spectra for the unknown compounds and polymers in this research are available in the Supporting Information.

TABLE 1 Molecular Weight and Thermal Properties of the Conjugated Polymers

	Target Polymer				
Polymer	M_w	M_n	PDI	T_d (°C)	T_g (°C)
CPDT-*co*-TPADCN	22,931	9410	2.44	425.6	44.7, 188.6
CPDT-*co*-TPADTA	9,816	5479	1.79	305.3	53.1, 202.9
CPDT-*co*-TPATCN	11,520	6947	1.66	385.8	54.7
CPDT-*co*-FADCN	32,879	11,260	2.92	422.4	53.2, 145.4
CPDT-*co*-FADTA	9,970	4409	2.26	308.5	56.7, 149.8
CPDT-*co*-FATCN	15,639	6807	2.30	418	55.6, 161.5

Thermal Properties

The thermal properties of the conjugated polymers were measured by DSC and TGA under nitrogen atmosphere (Table 1). As shown in Figure 1, the decomposition temperatures (T_d) of all the polymers are >300 °C, which indicates the excellent thermal stability of these polymers. It is interesting to note that all the polymers except **CPDT-*co*-TPATCN** exhibited two glass transition temperatures (T_g). The first T_g ranging from 44.7 to 56.7 °C reflects the conformational fluctuation on the polymer main chains. It is found that as the electron-withdrawing ability of the acceptors increases (TCN > DTA > DCN), the second T_g is increased in both the TPA-based polymers and DFA-based polymers. The stronger acceptor results in the larger dipole moment of the dye, thereby enhancing the intermolecular electrostatic interaction. Accordingly, more thermal energy is needed to induce the side chain movement, and higher second T_g values were observed in DSC measurement.

Optical Properties

The UV–vis absorption characteristics of the polymers were measured in both dilute toluene solutions (Fig. 2) and in spin-coated films (Fig. 3) with the relevant optical parameters

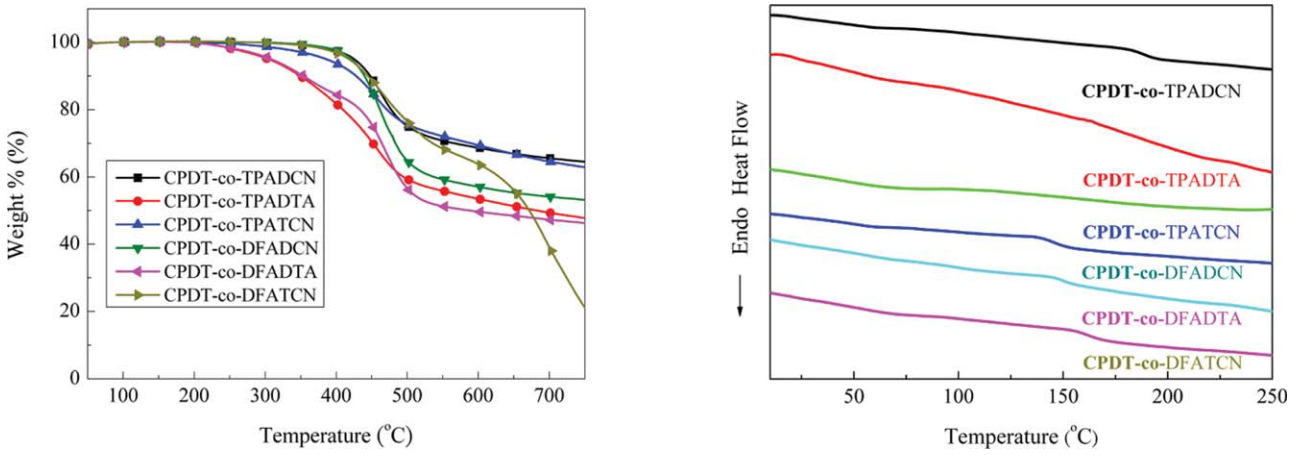

FIGURE 1 (a) TGA and (b) DSC measurement of the six conjugated polymers. [Color figure can be viewed in the online issue, which is available at wileyonlinelibrary.com.]

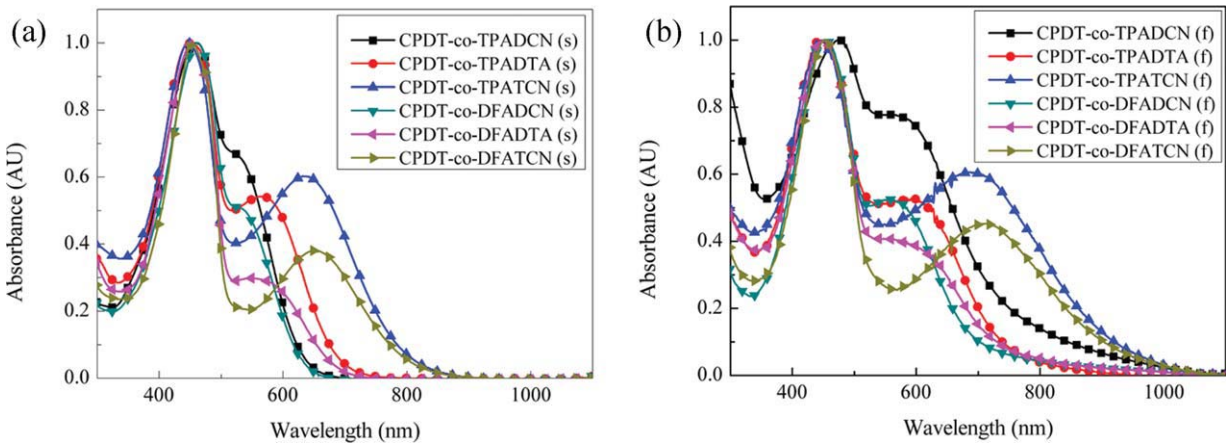

FIGURE 2 UV–vis absorption spectra of the conjugated polymers in the THF solution (a) and in the solid film (b).

summarized in Table 2. All the polymers exhibit two distinct absorption bands. The first absorption peak at the shorter wavelength is attributed to the π–π^* transition of the conjugated main chain and the second band at the longer wavelength comes from the ICT from the donor to the acceptor in the side chain chromophore. All the TPA-based polymers in THF solution show similar absorption maximum (λ_{max}) of the π–π^* transition band. However, the λ_{max} of the ICT band is significantly red shifted from 522 nm for **CPDT-*co*-TPADCB** to 566 nm for **CPDT-*co*-TPADTA** and to 632 nm for **CPDT-*co*-TPATCN**. The optical band-gap of the TPA-based polymers deduced from the absorption band edge also follows the same trend (1.7 eV for **CPDT-*co*-TPADCN**, 1.69 eV for **CPDT-*co*-TPADTA** and 1.34 eV for **CPDT-*co*-TPATCN**). Similar phenomena can also be observed in the DFA-based polymers. These results clearly reveal that the withdrawing ability of the acceptor is in the following order: TCN > DTA > DCN. The more powerful the acceptor the easier the charge separation, leading to the more red shifted ICT band and smaller optical band-gaps (E_g^{opt}). It is also interesting to note that the ICT band in each polymer is significantly red shifted by approximately 30–50 nm from the solution to the solid state, whereas the π–π^* transition absorption band remains essentially unchanged. This result indicates the strong dipole–dipole electrostatic interaction between the dipolar D–π–A chromophores in the solid state. When compared with the TPA-based polymer, the corresponding DFA-based polymer analogues have stronger intensity in the π–π^* transition bands due to the extra absorption of the fluorene groups.

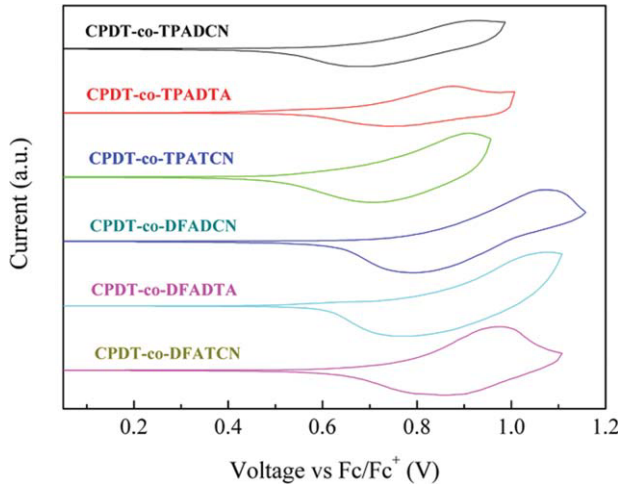

FIGURE 3 CV of the conjugated polymers in the thin film at a scan rate of 50 mV/s. [Color figure can be viewed in the online issue, which is available at wileyonlinelibrary.com.]

Electrochemical Properties

The CV of the six conjugated polymers is shown in Figure 3, and their electrochemical properties including oxidation potentials (E_{ox}^{onset}), HOMO, and LUMO levels of the polymers are summarized in Table 3. The HOMO energy levels of the TPA-based polymers are estimated to be from −5.06 to −5.08 eV with very small variations, whereas the DFA-based polymers exhibit lower-lying HOMO energy levels ranging from −5.17 to −5.21 eV. This result indicates that the HOMO energy level is mainly determined by the chemical environment of the amino groups that link the polymer main chain with the side chain. The LUMO energy levels were approximately estimated by subtracting the band-gap values from the corresponding HOMO levels. As the electron withdrawing strength of the acceptor increases, deeper LUMO level was found (LUMO: **CPDT-*co*-TPATCN** > **CPDT-*co*-TPADTA** >

TABLE 2 Optical Properties of the Conjugated Polymers

	λ_{max} (nm)		
Polymer	Solution (in THF)	Film	E_g^{opt} (eV)
CPDT-*co*-TPADCN	458, 522	476, 558	1.70
CPDT-*co*-TPADTA	451, 566	445, 594	1.69
CPDT-*co*-TPATCN	446, 632	447, 687	1.34
CPDT-*co*-FADCN	461, 525	452, 557	1.80
CPDT-*co*-FADTA	453, 546	450, 580	1.69
CPDT-*co*-FATCN	453, 651	452, 708	1.34

TABLE 3 Electrochemical Properties of the Conjugated Polymers

Polymer	E_{ox}^{onset} (V)	HOMO[a] (eV)	LUMO[b] (eV)
CPDT-*co*-TPADCN	0.68	−5.08	−3.38
CPDT-*co*-TPADTA	0.66	−5.06	−3.37
CPDT-*co*-TPATCN	0.65	−5.06	−3.72
CPDT-*co*-FADCN	0.80	−5.20	−3.40
CPDT-*co*-FADTA	0.80	−5.21	−3.52
CPDT-*co*-FATCN	0.76	−5.17	−3.83

[a] The HOMO energy levels were obtained from the equation HOMO = $-(4.8 + E_{ox}^{onset})$.
[b] The LUMO levels were calculated from the equation LUMO = HOMO + E_g^{opt}.

CPDT-*co*-TPADCN and **CPDT-*co*-DFATCN** > **CPDT-*co*-DFADTA** > **CPDT-*co*-DFADCN**). Apparently, the more powerful the acceptor on the side chain, the higher the electron affinity that finally leads to the deeper-lying LUMO level in these polymers. The HOMO–LUMO energy diagram of the polymers is shown in Figure 4. It should be noted that **CPDT-*co*-TPATCN** and **CPDT-*co*-DFATCN** polymers exhibit relatively low LUMO levels (−3.72 and −3.83 eV, respectively) that turns out to be lower than the LUMO level of $PC_{71}BM$ (−3.8 eV), which will reduce the efficiency of charge transfer from polymers to PCBM.

Photovoltaic Characteristics

BHJ solar cell devices were fabricated on the basis of ITO/PEDOT:PSS/polymer:$PC_{71}BM$ (1:4)/Ca/Al configuration, and the characteristics were measured under AM1.5 illumination at 100 mW/cm^2. $PC_{71}BM$ was used as the acceptor because it exhibited stronger absorption in the visible region than that of $PC_{61}BM$ ([6,6]-phenyl-C_{61}-butyric acid methyl ester).[40,41] The photovoltaic data are summarized in Table 4, and the *J*–*V* curves of these polymers are shown in Figure 5. The polymers **CPDT-*co*-TPATCN** and **CPDT-*co*-DFATCN** incorporating the TCN acceptor in the dyes exhibit broader absorption spectra to enhance light harvesting ability. Unfortunately, the strong electron-accepting strength of TCN also makes the polymers' LUMO energy levels lower than that of $PC_{71}BM$, which prohibits favorable electron transfer from the polymers to the $PC_{71}BM$. Consequently, the devices based on the **CPDT-*co*-TPATCN** and **CPDT-*co*-DFATCN** exhibited the relatively low PCEs of 0.22 and 0.31%, respectively. However, photovoltaic performances of devices based on **CPDT-*co*-TPATCN** and **CPDT-*co*-DFATCN** polymers are expected to be improved, if an n-type material possessing much lower-lying LUMO energy level than that of $PC_{71}BM$ is used for favorable charge transfer. From Table 4, the V_{oc} of the DFA-based conjugated polymers are higher than that of the corresponding TPA-based conjugated polymers. This improvement is attributed to the deeper-lying HOMO energy levels of the DFA-based polymers. The devices based on **CPDT-*co*-DFADCN**:$PC_{71}BM$ blend and **CPDT-*co*-DFADTA**:$PC_{71}BM$

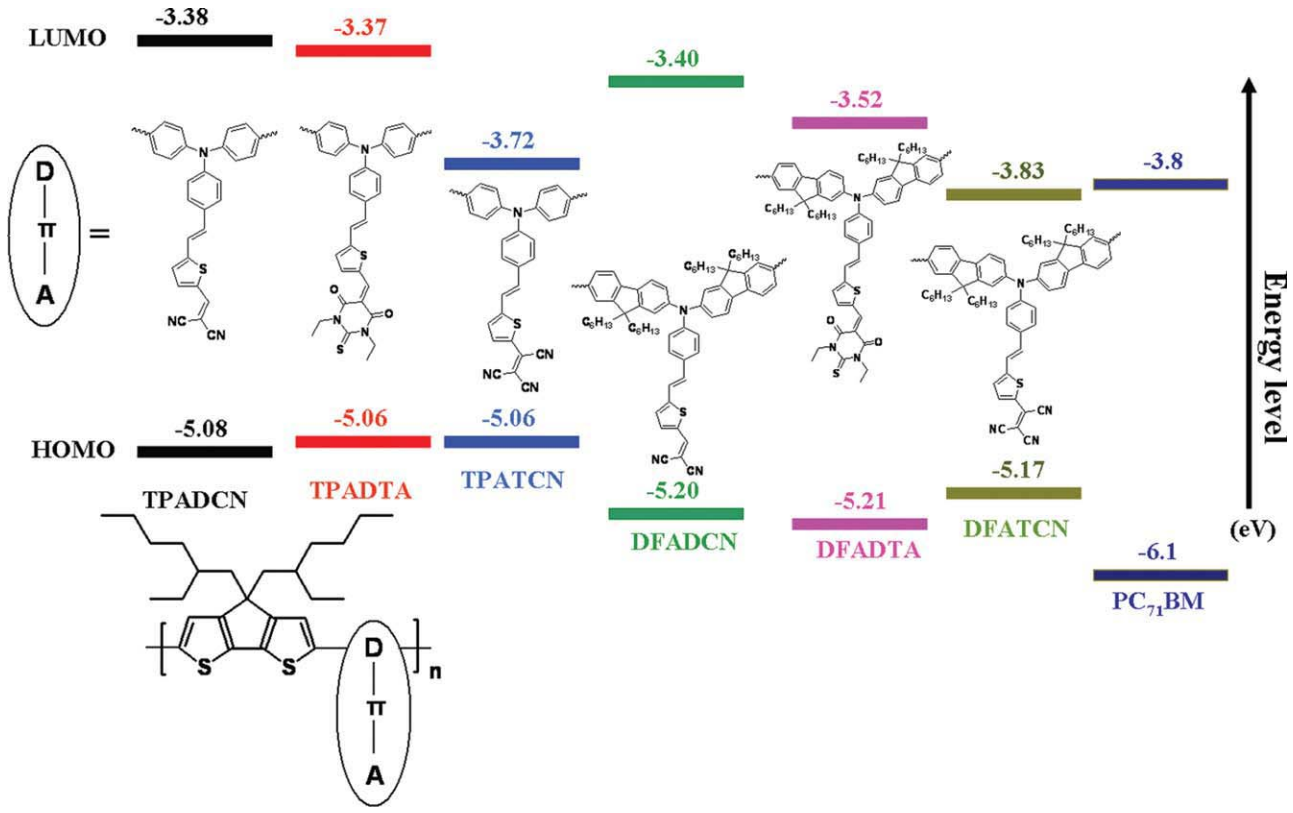

FIGURE 4 HOMO–LUMO energy diagram of the six conjugated polymers. [Color figure can be viewed in the online issue, which is available at wileyonlinelibrary.com.]

TABLE 4 Photovoltaic Performance of the Conjugated Polymers Obtained Under the Illumination of Simulated AM 1.5 G Conditions (100 mW/cm^2)

Polymer	Wt % Ratio of Polymer and $PC_{71}BM$	Hole Mobility (cm^2/V s)	V_{oc} (V)	J_{sc} (mA/cm^2)	FF	PCE (%)
CPDT-*co*-TPADCN	1:4	4.8×10^{-5}	0.64	4.45	0.40	1.14
CPDT-*co*-TPADTA	1:4	5.4×10^{-5}	0.62	4.65	0.41	1.18
CPDT-*co*-TPATCN	1:4	7.4×10^{-6}	0.58	1.26	0.32	0.22
CPDT-*co*-DFADCN	1:4	5.8×10^{-5}	0.79	3.51	0.49	1.36
CPDT-*co*-DFADTA	1:4	6.8×10^{-5}	0.70	4.57	0.43	1.38
CPDT-*co*-DFATCN	1:4	8.7×10^{-6}	0.70	1.17	0.38	0.31

blend achieved the PCE of 1.36 and 1.38%, respectively, which are slightly higher than the corresponding devices based on **CPDT-*co*-TPADCN**:PCBM blend (PCE = 1.14%) and **CPDT-*co*-TPADTA**:PCBM blend (PCE = 1.18%). This result also indicates that DTA is the most optimal acceptor. To estimate the hole mobilities of the polymers by space-charge limit current theory, the hole-only devices with the configuration of ITO/PEDOT:PSS/polymer/Au were fabricated. The hole mobilities of both the TPA and DPA-based polymers follow the same order: **CPDT-*co*-TPADTA** > **CPDT-*co*-TPADCN** > **CPDT-*co*-TPATCN**; **CPDT-*co*-DFADTA** > **CPDT-*co*-DFADCN** > **CPDT-*co*-DFATCN** (Table 4). This result is in good agreement and highly associated with the trend of the J_{sc} and PCEs in their corresponding devices.

CONCLUSIONS

We report a series of alternating copolymers incorporating coplanar CPDT unit in the main chain and D–π–A organic dyes in the side chain. The absorption spectrum, optical band-gap and HOMO–LUMO energy level of the conjugated polymers can be easily tailored by adjusting the electronic properties of the donor and the acceptor in the dye. It is found that the electron-withdrawing ability of the acceptor is in the following order: TCN > DTA > DCN. Because of the strongest accepting ability of TCN to induce efficient ICT, **CPDT-*co*-TPATCN** and **CPDT-*co*-DFATCN** exhibit the broader absorption spectra covering from 400 to 900 nm and the narrower optical band gaps of 1.34 eV. However, the stronger electron-accepting strength also significantly lowers the LUMO energy level of **CPDT-*co*-TPATCN** and **CPDT-*co*-DFATCN** to −3.72 and −3.83 eV, respectively. The **CPDT-*co*-TPATCN**:$PC_{71}BM$ and **CPDT-*co*-DFATCN**:$PC_{71}BM$ based solar cells exhibited the PCEs of 0.22 and 0.31%, respectively, due to the inefficient exciton dissociation. The DFA-based polymers possess deeper-lying HOMO energy levels than the TPA-based polymer analogues, leading to the higher V_{oc} values and thereby better efficiencies. The device based on **CPDT-*co*-DFADTA**:$PC_{71}BM$ blend achieved the best PCE of 1.38% with a V_{oc} of 0.7 V, a J_{sc} of 4.57 mA/cm^2, and a fill factor of 0.43.

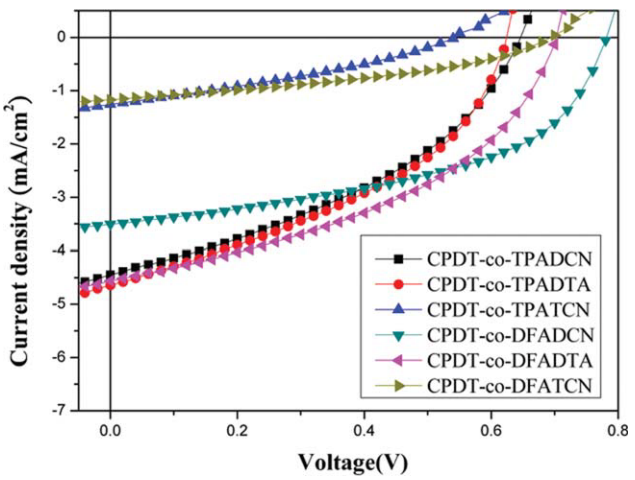

FIGURE 5 *J–V* characteristics of ITO/PEDOT:PSS/polymer:$PC_{71}BM$/Ca/Al under illumination of AM1.5 solar simulator at 100 mW/cm^2. [Color figure can be viewed in the online issue, which is available at wileyonlinelibrary.com.]

This work is supported by the National Science Council and "ATU Plan" of the National Chiao Tung University and Ministry of Education, Taiwan.

REFERENCES AND NOTES

1 Brabec, C. J.; Sariciftci, N. S.; Hummelen, J. C. Adv Funct Mater 2001, 11, 15–26.

2 Günes, S.; Neugebauer, H.; Sariciftci, N. S. Chem Rev 2007, 107, 1324–1338.

3 Cheng, Y. J.; Yang, S. H.; Hsu, C. S. Chem Rev 2009, 109, 5868–5923.

4 Yu, G.; Gao, J.; Hummelen, J. C.; Wudl, F.; Heeger, A. J. Science 1995, 270, 1789–1791.

5 Thompson, B. C.; Fréchet, J. M. J. Angew Chem Int Ed 2008, 47, 58–77.

6 Hummelen, J. C.; Knight, B. W.; LePeg, F.; Wudl, F. J Org Chem 1995, 60, 532–538.

7 Brabec, C. J.; Cravino, A.; Meissner, D.; Sariciftci, N. S.; Fromherz, T.; Rispens, M. T. Sanchez, L.; Hummelen, J. C. Adv Funct Mater 2001, 11, 374–380.

8 Lenes, M.; Wetzelaer, G.-J. A. H.; Kooistra, F. B.; Veenstra, S. C.; Hummelen, J. C.; Blom, P. W. M. Adv Mater 2008, 20, 2116–2119.

9 Kooistra, F. B.; Knol.J.; Kastenberg, F.; Popescu, L. M.; Verhees, W. J. H.; Kroon, J. M.; Hummelen, J. C. Org Lett 2007, 9, 551–554.

10 Brabec, C. J.; Winder, C.; Sariciftic, N. S.; Hummelen, J. C.; Dhanabalan, A.; van Hal, P. A.; Janssen, R. A. J. Adv Func Mater 2002, 12, 709–712.

11 Halls, J. J. M.; Cornil, J.; dos Santos, D. A.; Silbey, R.; Hwang, D.-H.; Holmes, A. B.; Brédas, J. L.; Friend, R. H. Phy Rev B 1999, 60, 5721–5727.

12 Huo, L.; Hou, J.; Zhang, S.; Chen, H.-Y.; Yang, Y. Angew Chem Int Ed 2010, 49, 1500–1503.

13 Hou, J.; Chen, H.-Y.; Zhang, S.; Li, G.; Yang, Y. J Am Chem Soc 2008, 130, 16144–16145.

14 Zou, Y.; Naiari, A.; Berrouard, P.; Beaupre, S.; Aich, B. R.; Tao, Y.; Leclerc, M. J Am Chem Soc 2010, 132, 5330–5331.

15 Liang, Y.; Wu, Y.; Feng, D.; Tsai, S.-T.; Son, H.-J.; Li, G.; Yu, L. J Am Chem Soc 2009, 131, 56–57.

16 Qin, R.; Li, W.; Li, C.; Du, C.; Veit, C.; Schleiermacher, H.-F.; Adersson, M.; Bo, Z.; Liu, Z.; Inganas, O.; Wuerfel, U.; Zhang, F. J Am Chem Soc 2009, 131, 14612–14613.

17 Chen, H.-Y.; Hou, J.; Zhang, S.; Liang, Y.; Yang, G.; Yang, Y.; Yu, L.; Wu, Y.; Li, G. Nat Photon 2009, 3, 649–653.

18 Hou, J.; Chen, H.-Y.; Zhang, S.; Chen, R. I.; Yang, Y.; Wu, Y.; Li, G. J Am Chem Soc 2009, 131, 15586–15587.

19 Park, S. H.; Roy, A.; Beaupre, S.; Cho, S.; Coates, N.; Moon, J. S.; Moses, D.; Leclerc, M.; Lee, K.; Heeger, A. J. Nat Photon 2009, 3, 297–302.

20 Liang, Y.; Xu, Z.; Xia, J.; Tsai, S.-T.; Wu, Y.; Li, G.; Ray, C.; Yu, L. Adv Mater 2010, 22, E135–E138.

21 Wang, E.; Wang, L.; Lan, L.; Luo, C.; Zhuang, W.; Peng, J.; Cao, Y. Appl Phys Lett 2008, 92, 033307.

22 Dalton, L. R.; Sullivan, P. A.; Bale, D. H. Chem Rev 2010, 110, 25–55.

23 Marks, T. J.; Ratner, M. A. Angew Chem Int Ed 1995, 34, 155–173.

24 Cheng, Y.-J.; Luo, J.; Hau, S.; Bale, D. H.; Kim, T.-D.; Shi, Z.; Lao, D. B.; Tucker, N. M.; Tian, Y.; Reid, P. J.; Dalton, L. R.; Jen, A. K-Y. Chem Mater 2007, 19, 1154–1163.

25 Cheng, Y.-J.; Luo, J.; Huang, S.; Zhou, X.-H.; Shi, Z.; Kim, T.-D.; Bale, D. H.; Takahashi, S.; Yick, A.; Polishak, B. M.; Jang, S.-H.; Reid, P. J.; Dalton, L. R.; Steier, W. H.; Jen, A. K.-Y. Chem Mater 2008, 20, 5047–5054.

26 Chen, K.-F.; Hsu, Y.-C.; Wu, Q.; Yeh, M.-C. P.; Sun, S.-S. Org Lett 2009, 11, 377–380.

27 Teng, C.; Yang, X.; Yang, C.; Tian, H.; Li, S.; Wang, X.; Hagfeldt, A.; Sun, L. J Phys Chem C 2010, 114, 11305–11313.

28 Im, H.; Kim, S.; Park, C.; Jang, S.-H.; Kim, C.-J.; Kim, K.; Park, N.-G.; Kim, C. Chem Commun 2010, 46, 1335–1337.

29 Tian, H.; Yang, X.; Pan, J.; Chen, R.; Liu, M.; Zhang, Q.; Hagfeldt, A.; Sun, L. Adv Funct Mater 2008, 18, 3461–3468.

30 Erten-Ela, S.; Yilmaz, M. D.; Icli, B.; Dede, Y.; Icli, S.; Akkaya, E. U. Org Lett 2008, 10, 3299–3302.

31 Qin, P.; Zhu, H.; Edvinsson, T.; Boschloo, G.; Hagfeldt, A.; Sun, L. J Am Chem Soc 2008, 130, 8570–8571.

32 Huang, F.; Chen, K.-S.; Yip, H.-L.; Hau, S. K.; Acton, O.; Zhang, Y.; Luo, J.; Jen, A. K.-Y. J Am Chem Soc 2009, 131, 13886–13887.

33 Duan, C.; Cai, W.; Huang, F.; Zhang, J.; Wang, M.; Yang, T.; Zhong, C.; Gong, X.; Cao, Y. Macromolecules, 2010, 43, 5262–5268.

34 Duan, C.; Chen, K.-S.; Huang, F.; Yip, H.-L.; Liu, S.; Zhang, J.; Jen, A. K.-Y.; Cao, Y. Chem Mater 2010, 22, 6444–6452.

35 Zhang, Z.-G.; Liu, Y.-L.; Yang, Y.; Hou, K.; Peng, B.; Zhao, G.; Zhang, M.; Guo, X.; Kang, E.-T.; Li, Y. Macromolecules 2010, 43, 9376–9383.

36 Hsu, S.-L.; Chen, C.-M.; Wei, K.-H. J Polym Sci Part A: Polym Chem 2010, 48, 5126–5134.

37 Coppo, P.; Turner, M. L. J Mater Chem 2005, 15, 1123–1133.

38 Zhu, Z.; Waller, D.; Gaudiana, R.; Morana, M.; Mühlbacher, D.; Scharber, M.; Brabec, C. Macromolecules 2007, 40, 1981–1986.

39 Woo, H. Y.; Shim, H.-K.; Lee, K.-S. Synth Met 1999, 101, 136–137.

40 Wienk, M. M.; Kroon, J. M. Verhees, W. J. H.; Knol, J.; Hummelen, J. C.; van Hal, P. A.; Janssen, R. A. J. Angew Chem Int Ed 2003, 42, 3371–3375.

41 Yao, Y.; Shi, C.; Li, G.; Shrotriya, V.; Pei, Z.; Yang, Y. Appl Phys Lett 2006, 89, 153507.